Coils and Compensation Circuit Design Reduces Power Pulsation and Optimizes Transfer Efficiency in the Dynamic Wireless Charging System for Electric Vehicles

Nguyen Thi Diep[1], Tran Trong Minh[2], Nguyen Kien Trung[2],*

[1]*Electric Power University, Hanoi, Vietnam*
[2]*Hanoi University of Science and Technology, Hanoi, Vietnam*
Email: trung.nguyenkien1@hust.edu.vn,

Abstract

This paper presents a method of designing coils and compensation circuits to reduce output power pulsation, optimize transfer efficiency for electric vehicle dynamic wireless charging systems. The transmission lane is modularly designed. Each module has three short-track transmitter coils that are placed closely together along the moving track of the receiver and connected to a single inverter. The designs of the transmitter and receiver coils are analyzed by finite element analysis to reduce the variation of the coupling coefficient. Then the coupling coefficient is analyzed to identify the characteristics of the dynamic wireless charging lane. The double-sided LCC compensation circuit is designed according to the optimum load value to obtain maximum transfer efficiency. The SIC devices are used to improve the efficiency of the 85 kHz resonant inverter. A 1.5 kW dynamic charging system prototype is constructed. Experimental results show that the average system efficiency of 89.5% is obtained, and the output power pulse rate is ±9.5% in the dynamic charging process.

Keywords: Electric vehicle, dynamic wireless charging, LCC compensation circuit.

1. Introduction

In recent years, electric vehicles are an efficient and increasingly popular green energy vehicle in the world. Wireless charging system for electric vehicles based on wireless power transfer (WPT) technology intense research and development [1]. Currently, dynamic wireless charging systems are attracting system researchers and developers. This system has the characteristic that the vehicle is continuously charged while moving. Therefore, the travel distance is longer, and the capacity and weight of the battery are less [2].

In today's dynamic charging system designs, the short-track transmission lane structure is often used because of its high efficiency and low electromagnetic interference [3], [4]. However, this structure is complex. It requires a large number of compensating circuits, power converters, and vehicle position detectors. Furthermore, the output power is pulsed [5], [6]. In this paper, a short-track transmission lane structure is proposed to be designed by the finite element analysis (FEA) method to reduce the change of coupling coefficient when the vehicle is moving. Therefore, the output power pulsation is reduced.

In the WPT system, the energy is transmitted through the air. Therefore, the coupling coefficient is small, and the transfer efficiency is low [1]. Resonance is the key for a WPT system to transmit power with high power and high efficiency. Compensation circuits are used to create the resonant circuit in the WPT system. At the kHz frequency range, the resonant circuit is created by adding compensating capacitors to the circuit. There are four basic compensating structures: Series – Series, Series-Parallel, Parallel–Series, Parallel–Parallel structure [7]. The advantages of these compensating circuits are simplicity and ease of design. The disadvantage of these is sensitivity to variations in parameters, and the power and efficiency characteristics are decoupled when the load changes. The LCC compensation circuit structure has many advantages such as high efficiency, the small size of circuit parameters [8], soft-switching condition, and the resonance frequency are independent of the coefficient coupling, load [9]. Therefore, it is suitable for the dynamic wireless charging system. Besides, the WPT system is featured by its maximum transfer efficiency at a specified value of the load which is called the optimal impedance load value [10], [11], [12]. Therefore, in this paper, the double-side LCC compensation circuit is proposed to be designed according to the optimal impedance load value to maximize the transfer efficiency in the dynamic wireless charging system. Furthermore, the compensating circuit is designed considering the coefficient coupling between the transmitter coils. An experimental prototype of a dynamic wireless charging system is built to verify the accuracy of the proposed method.
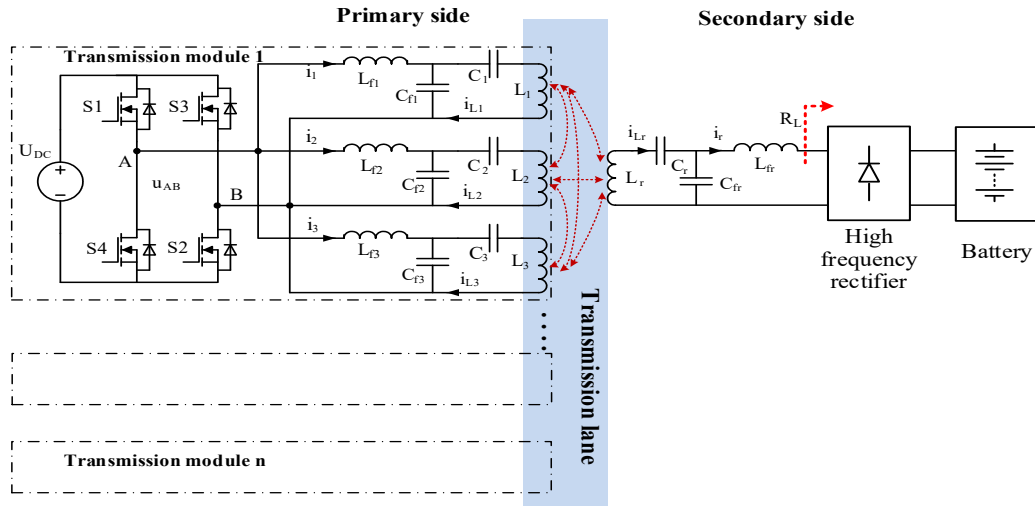
Fig. 1. System structure diagram.

The paper structure consists of the following section: section 2 presents the system design, section 3 presents simulation and experimental results, the conclusions are summarized in section 4.

2. Design System

2.1. Sysem Structure Design

The proposed system structure is as shown in Fig. 1, the transmission lane is designed in short-track and is modularized. The primary side consists of multiple transmission modules. Each transmission module includes an inverter that powers three coils, where each coil is connected to a separate LCC compensation circuit. This structure on the primary side has the following advantages: The transmission modules can be controlled on/off according to the position of EV which increases efficiency and reduces electromagnetic interference. We can easily extend the transmission lane without changing the design. Also, it is easy to design compensation capacitors.

On the primary side, the DC input voltage is converted into a high-frequency AC voltage by a single-phase bridge inverter. And then, through the LCC compensation circuit, high-frequency AC voltage is fed to the transmitting coils. On the secondary side, the AC voltage received on the receiving coil through to the LCC compensation circuit is rectified to DC voltage by a high-frequency rectifier. In this paper, the problem of switching between transmission modules is not considered. We don't consider the control problem of the secondary power converters. Therefore, replace the secondary side looking from the rectifier to the load with an equivalent load impedance R_L.

2.1. Coil Design Reducing Output Power Pulsation

In this section, the design method of the magnetic coupler by simulation of FEA on Ansys Maxwell software is presented to reduce the fluctuation of the coupling coefficient when the EV moves to reduce the power pulsation. Then, the characteristic of the coupling coefficient when the EV moves lateral misalignment is analyzed to clarify the characteristics of the transmission lane.
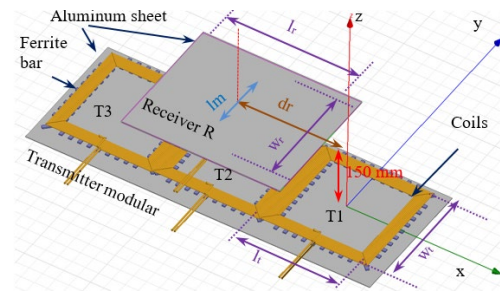

Fig. 2. Maxwell 3D model of a magnetic coupler module

The magnetic coupler structure of one transmission module is designed as shown in Fig. 2. The magnetic coupler is designed with three layers. The first layer is rectangular monopole coils. The second layer is ferrite rods placed below the coils to conduct magnetism and strengthen the electromagnetic connection between the transmitting and receiving coils. The third layer is the aluminum shield that affects shielding the leakage of the magnetic field to the environment. On the primary side, each transmission module consists of three coils, and placed close together. The number of transmitting coils in a module is chosen to be three which is enough to reflect the mutual inductance between the transmitting coils in a dynamic charging system.

The thicknesses of the monopole coils, ferrite rods, and aluminum shields are designed to be 4.8 mm, 5 mm, and 2 mm, respectively. The ferrite layer is placed close to the monopole coils, and the aluminum shield is placed 25 mm from the ferrite layer. The distance between transmitter and receiver is designed to be 150 mm. Because of the limited space, each coil of the transmitter is designed with a fixed size.

Therein, the length (l_t) is 400 mm, and the width (w_t) is 400 mm, the number of turns is 10. The displacement of the receiver in the *x*-axis is defined as *dr,* when the receiver R is in a centered position with the first transmitter T1, *dr* is zero. The *y*-axis side offset is defined as *lm*, when the receiver R moves in the *x*-axis direction, *lm* is zero.

The receiver coupler is designed to have the same structure as the transmitters. The width of the receiving coil is fixed and equal to 400 mm. The length of the receiving coil is selected through FEA simulation

The coupling coefficients of the transmitting coils T1, T2, T3 with the receiving coil R are defined as k_{1r}, k_{2r}, k_{3r}. With $k_{1r} = M_{1r}/\sqrt{L_1 L_r}$; $k_{2r} = M_{2r}/\sqrt{L_2 L_r}$; $k_{3r} = M_{3r}/\sqrt{L_3 L_r}$; and L_1, L_2, L_3, L_r is the inductance of the transmitting and receiving coils, respectively. M_{1r}, M_{2r}, M_{3r} is the mutual inductance of transmitting coils (T1, T2, T3) with receiving coil (R).

The total coupling coefficient of the three transmitting coils to the receiving coil is calculated as follows:

$$k_r = k_{1r} + k_{2r} + k_{3r} \qquad (1)$$

Fig. 3a is the FEA simulation results of the total coupling coefficient in the three survey cases. Case 1: (the length of the receiving coil is equal to the length of the transmitting coil) $l_r = l_t = 400$ mm. Case 2: $l_r = 1.25l_t = 500$ mm. Case 3: $l_r = 1.5l_t = 600$ mm. When the receiver moves along the transmission lane, *dr* changes from 0 mm to 800 mm and *lm* = 0mm. The results show that the total coupling coefficient varies according to the receiver position. The average value of the total coupling coefficient in the three cases is equal to 0.128, 0.140, and 0.165, respectively. The variation of the total coupling coefficient in the three cases is equal to 9.9%, 6%, 9.6%, respectively. Thus, when the length of receiving coil increases, the total coupling coefficient increases. However, the variation of the total coupling coefficient changes is not proportional to the length of the receiver. In the survey cases, the variation of the total coupling coefficient is lowest in case 2, so this case is chosen to design the receiver.

The results of the FEA simulation of the coupling coefficients of each transmitting coil with the receiving coil in the design case are shown in Fig. 3b. The coupling coefficients of each transmitting coil with the receiving coil are maximum when the position of the receiving coil is centered with that transmitting coil and are smaller when the receiving coil is located far from that transmitting coil. At position *dr* = 0 mm, *lm* = 0 mm, receiver R is centered with transmitter T1, the coupling coefficients have the following values: $k_{1r} = 0.18755$, $k_{2r} = -0.03343$, $k_{3r} = -0.01291$.
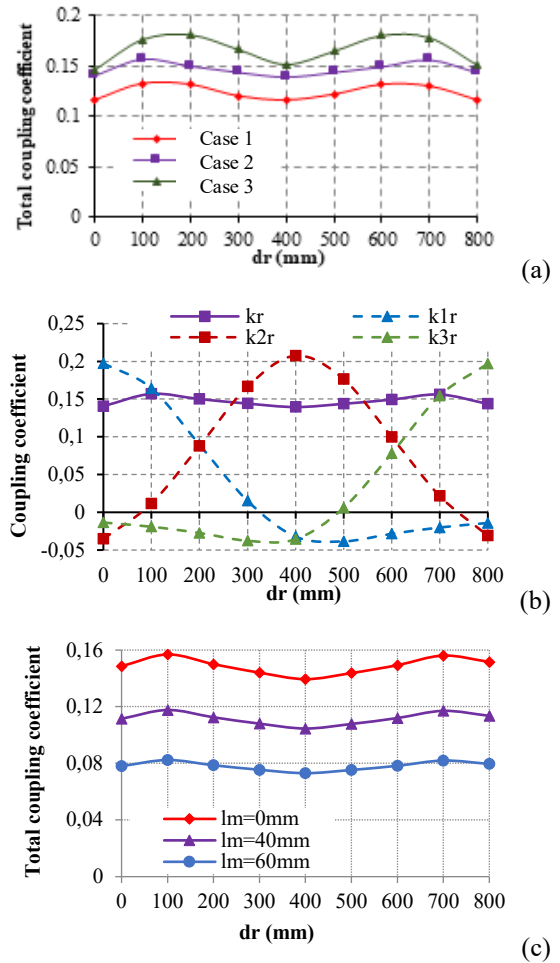

Fig. 3. FEA simulation results. a) Total coupling coefficient, b) Component coupling coefficients in case l_r=500 mm, c) Total coupling coefficients in case EV moves lateral misalignment

When the receiver moves with lateral misalignment, the FEA simulation results of the total coupling coefficient is shown in Fig. 3c. The results show that when the receiver moves with lateral misalignment in the *y*-direction *lm* = 40 mm, *lm* = 60 mm (respectively 20%, 30%), the total coupling coefficient reduces to 0.111, 0.78, respectively. Thus, the total coupling coefficient changes when the receiver moves along in the transmission lane, which decreases sharply when the receiver moves with lateral misalignment.

When the receiver position is *dr* = 0 mm, *lm* = 0 mm, the magnetic field simulation results are shown in Fig. 4. According to the 2010 ICNIRP standard, the required exposure limit for public places is 27µT at 85kHz. The simulation results show that the magnetic field emission of the designed system reaches a safe level at a distance of 400mm from the system.

FEA simulation results of inductance, mutual inductance, and connection coefficient of the magnetic

coupler on transmitting and receiving module are listed in Table 1.

Table 1. Magnetic coupler parameter

Parameter	Value	Parameter	Value
L_i (i=1÷3)	102 μH	L_r	120 μH
$M_{12} = M_{21}$	-10.183 μH	$M_{13} = M_{31}$	-1.754 μH
$M_{23} = M_{32}$	-10.183 μH	k_r	0.14

where, M_{ij} is the mutual inductance of ith transmitting coils with the jth transmitting coil. And i, j are the indices of the transmitting coils ($i, j = 1, 2, 3$, and $i \neq j$).
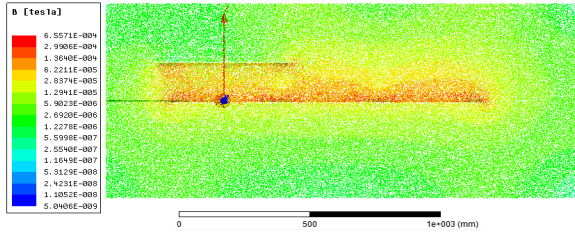

Fig. 4. Magnetic field emission in Ansys Maxwell simulations.

2.2. Compensation Circuit Design for Maximum Transfer Efficiency

In this section, the LCC compensation circuit is designed for both the transmitting and receiving sides. Because the electrical lengths of the wiring and coils are very short, the WPT system is analyzed according to a pooled parametric model. The equivalent circuit diagram is shown in Fig. 5. The electromagnetic coupling between the coils is represented by the induced voltages. Each transmitting coil is electromagnetically connected to the other two transmitting coils and the receiving coil. The receiving coil is electromagnetically connected to the three transmitting coils. The induced voltage in each coil depends on the value of the mutual inductance and the current in the other coil as Fig. 5.

The circuit diagram in Fig. 5 is a multi-source linear circuit. Therefore, the superposition method is used to analyze the circuit [8], and the characteristic of the circuit is analyzed at a constant resonant frequency f_0. For simplicity of analysis, the losses on coils and compensation circuits are ignored. The resonance relationship of the components of the double-side LCC compensation circuit is shown as follows:

$$
\begin{cases}
C_{fr} = \dfrac{1}{\omega^2 L_{fr}} \\
C_r = \dfrac{1}{\omega^2 [L_r - L_{fr}]} \\
C_{fi} = \dfrac{1}{\omega^2 L_{fi}} \\
C_i = \dfrac{1}{\omega^2 (L_i - L_{fi} + \sum_{k=1, k \neq i}^{3} M_{ik})}
\end{cases}
\tag{2}
$$

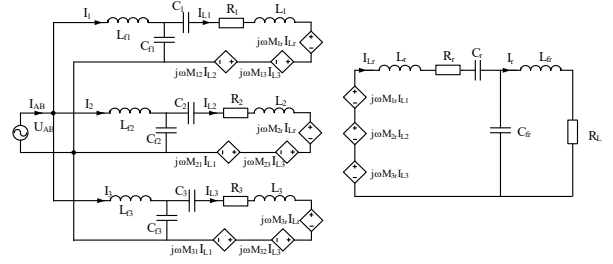where $\omega = 2\pi f_0$.

Fig. 5. Equivalent circuit diagram

At resonant condition, the resonant current in transmitting coils are same and equal to:

$$I_{L1} = I_{L2} = I_{L3} = I_{Li} = -j\omega C_{fi} U_{AB} \tag{3}$$

When considering the resistances of the transmitting and receiving coils, the transmitting coils are of the same design, so the values of the resistances are assumed to be equal and equal to R_i:

$$R_1 = R_2 = R_3 = R_i \tag{4}$$

Where, R_1, R_2, R_3, R_r are the resistances of the transmitting coils T1, T2, T3, and the receiving coil R, respectively.

The transfer efficiency can be expressed as:

$$
\begin{aligned}
\eta &= \frac{R_L I_r^2}{R_L I_r^2 + R_r I_{Lr}^2 + R_1 I_{L1}^2 + R_2 I_{L2}^2 + R_3 I_{L3}^2} \\
&= \frac{R_L}{R_L + R_r (I_{Lr}/I_r)^2 + 3 R_i (I_{Li}/I_r)^2}
\end{aligned}
\tag{5}
$$

On the secondary side, the Kirchhoff 2 equations are written as follows.

$$
\begin{cases}
(R_L + j\omega L_{fr}) I_r - \dfrac{1}{j\omega C_{fr}} (I_r - I_{Lr}) = 0 \\
\left(\dfrac{1}{j\omega C_r} + R_r + j\omega L_r\right) I_{Lr} + \dfrac{1}{j\omega C_{fr}} (I_r - I_{Lr}) \\
\quad - (j\omega M_{1r} I_{L1} + j\omega M_{2r} I_{L2} + j\omega M_{3r} I_{L3}) = 0
\end{cases}
\tag{6}
$$

Combining (6), (2), and (3), the following equations are derived:

$$
\begin{cases}
\dfrac{I_{Lr}}{I_r} = -\dfrac{R_L}{j\omega L_{fr}} \\
\dfrac{I_{Li}}{I_r} = \left(\dfrac{R_r R_L}{\omega^2 L_{fr}} + L_{fr}\right) / M_r
\end{cases}
\tag{7}
$$

with $M_r = M_{1r} + M_{2r} + M_{3r}$ and $M_r = k_r \sqrt{L_i L_r}$

Combining (7) and (5) get the following expression:

$$
\eta = \frac{R_L}{R_L + \dfrac{R_r}{\omega^2 L_{fr}^2} R_L^2 + 3 R_i \dfrac{\left(\dfrac{R_r R_L}{\omega^2 L_{fr}} + L_{fr}\right)^2}{L_i L_r k_r^2}}
\tag{8}
$$

If the coils and compensator have been designed, the system operates at a resonant frequency (ω), then the parameters of coils (L_r, L_i, R_r, R_i) and compensation circuit (L_{fr}) are fixed. At each receiver position, the coupling coefficient (k_r) is fixed. The equivalent load impedance (R_L) depends on the state of charge of the

battery. Therefore, the transfer efficiency is a function of R_L. The maximum efficiency is obtained by solving the following equations:

$$\begin{cases} \frac{\partial \eta}{\partial R_L} = 0 \\ \frac{\partial \eta^2}{\partial R_L^2} < 0 \end{cases} \tag{9}$$

The maximum transfer efficiency is determined by

$$\eta_{max} = \frac{k_r^2 Q_i Q_r}{\left(\sqrt{3} + \sqrt{3 + k_r^2 Q_i Q_r}\right)^2} \tag{10}$$

That is achieved at:

$$R_{L.opt} = \frac{\omega^2 L_{fr}^2}{R_r} \sqrt{\frac{3}{3 + k_r^2 Q_i Q_r}} \tag{11}$$

Where, $Q_i = \omega L_i / R_i$, $Q_r = \omega L_r / R_r$ are the quality factor of the transmitting and receiving coils. Thus, at each receiver position, the transfer efficiency reaches its maximum value only at one value of the load, which is called the optimal load value ($R_{L.opt}$).

The parameters of the LCC compensation circuit are calculated for a 1.5 kW dynamic charging system, resonant frequency 85 kHz, and satisfying the resonance conditions in (2), the optimal load condition in (11) for maximum efficiency. Since the designed magnetic coupler has a small fluctuation of the coupling coefficient as the receiver moves along the transmission lane, the coupling coefficient value is chosen to design the compensation circuit equal to the average value ($k_r = 0.14$). Compensation circuit parameters is shown in Table 2.

Table 2. Compensation circuit parameters

Parameter	Value	Parameter	Value
L_{fi}	52.6 µH	C_3	95 nF
C_{fi}	66.5 nF	L_{fr}	28.9 µH
C_1	93.7 nF	C_{fr}	120.9 nF
C_2	123.2 nF	C_r	38.5 nF

3. Simulation and Experimental Results

In this section, simulation and experimental models are built to verify the proposed designs. Efficiency and power evaluations are investigated from the DC input of the primary inverter to the output of the AC load equivalent R_L.

A simulation model built on Ansys Electronics software linked to the magnetic circuit model on Ansys Maxwell software is used to investigate the transfer efficiency characteristics of the system as shown in Fig. 6.

In the WPT system, the transfer efficiency depends on the load impedance and the coupling coefficient. Therefore, it is necessary to consider the influence of these parameters on transfer efficiency. Fig. 7a is a frequency characteristic of transfer efficiency when the value of the equivalent load impedance R_L increases from 15 Ω to 150 Ω and the receiver is at position 0mm ($k_{1r} = 0.18755$, $k_{2r} = -0.03343$, $k_{3r} = -0.01291$). The results show that the maximum transfer efficiency is in the case $R_L = R_{L.opt} = 53.33$ Ω. For other values of the equivalent load impedance, the transfer efficiency decreases and rapidly declines in the frequency region around 85 kHz. Fig. 7b is a frequency characteristic of transfer efficiency when the receiver position changes and the load impedance R_L is $R_{L.opt}$. The results show that the transfer efficiency characteristics almost overlap. Maximum value of transfer efficiency reached 94.6%, and the frequency range for high-transfer efficiency is from 83 kHz to 89 kHz.
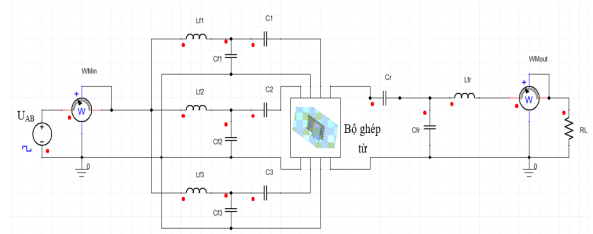
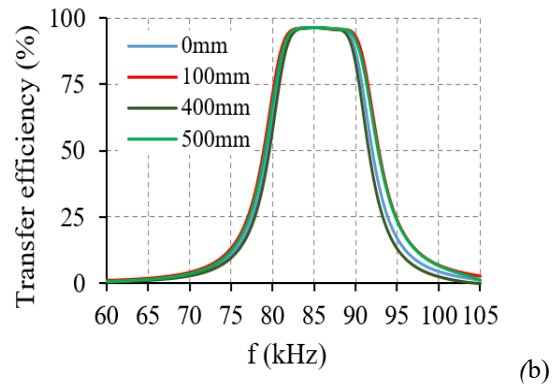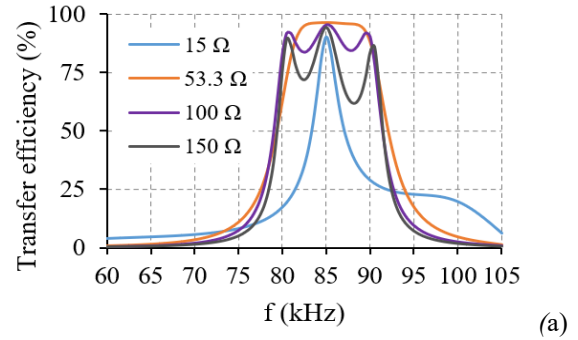Fig. 6. Simulation model on Ansys Electronics

(a)

(b)

Fig. 7. Frequency characteristic of transfer efficiency.
a) Case 1: *dr* = 0 mm, *lm* = 0 mm, R_L changes,
b) Case 2: $R_L = R_{L.opt}$, *lm* = 0 mm, *dr* changes

Table 3. Peak voltage and current stress

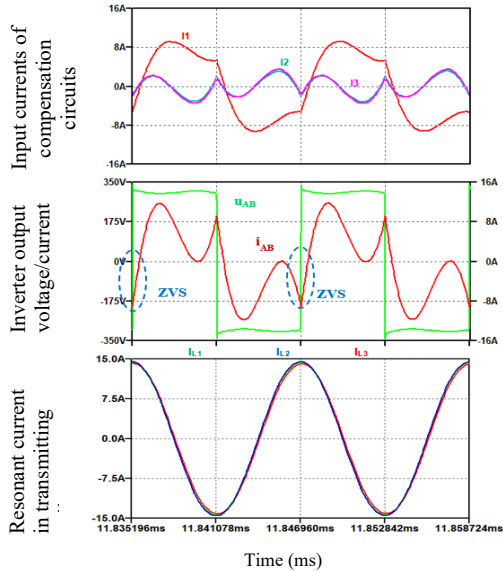| Parameter	Voltage	Current
MOSFET	340 V	11.78 A
C_{fi}	435 V	17.3 A
C_i	227 V	14.6 A
C_{fr}	408 A	26.1 A
C_r	1,1 kV	25 A

Fig. 8. Voltage and current waveforms in Ltspice simulation

Fig. 8 is simulation results of voltage/ current waveforms in the case of *dr* = 0 mm, *lm* = 0 mm by Ltspice model. In this position, the center of the receiver R is centered with the transmitter T1, so the current I_1 is largest and the currents I_2, I_3 are much smaller. From the simulation results of the voltage u_{AB} and the output current i_{AB} of the inverter, the ZVS soft-switching condition for the MOSFET is achieved. Resonant currents on transmitting coils I_{L1}, I_{L2}, I_{L3} are sinusoidal and in phase. The peak voltage and current stresses of the circuit components are shown in Table 3. MOSFETs achieve soft-switching, so the peak voltage is 340 V, the peak current stress is 11.78 A. For the compensation capacitors, the capacitor C_r has the highest voltage stress (1.1 kV) and the capacitor C_{fr} has the highest current stress (26.1 A).

Fig. 9 is an experimental model in the laboratory. The coils are built-in Stranded wire. The polypropylene film capacitors are used to reduce losses and increase the bearing capability at high currents in high frequencies. CMF20120D SIC MOSFETs are used to increase inverter efficiency.

Experimental results waveform output voltage/current of the inverter are shown in Fig. 10a. This voltage/current waveform is the same as the simulation result shown in Fig. 8. In addition, this

result also shows that ZVS soft-switching condition for MOSFET is achieved. The peak voltage is 328 V, the peak current stress is 12.8 A, I_{off} is 9.2 A, the inverter's output frequency is 85 kHz equal to the design frequency. Fig. 10b shows the voltage waveform on the optimal load, the output voltage frequency is also 85 kHz.
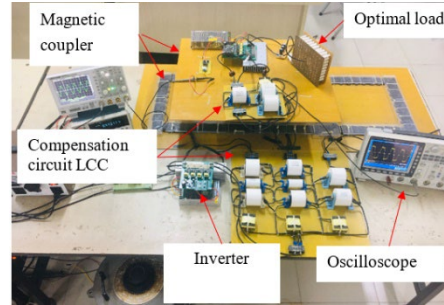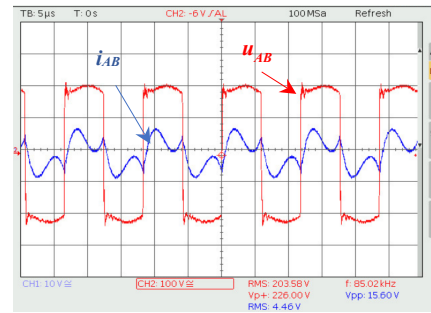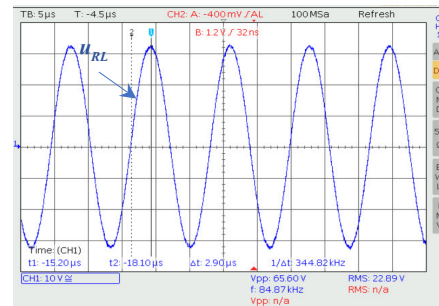

Fig. 9. Experimental model

(a)

(b)

Fig. 10. Experimental results of voltage/current waveform. a) Inverter output voltage/current, b) Optimal load voltage
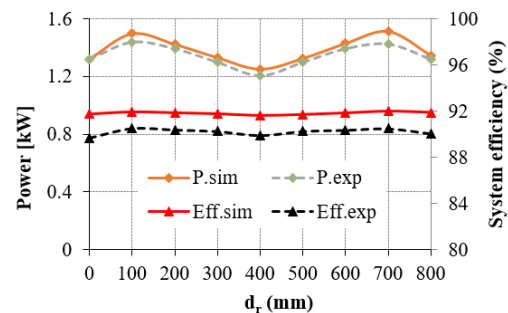

Fig. 11. Simulation/experimental results of power and system efficiency

Fig. 11 is the simulation Ltpice (solid line) and experimental (dot line) results of the output power and system efficiency. When the receiver moves along the transmission lane (*lm* = 0 mm, *dr* changes from 0 mm to 800 mm), the corresponding simulation and experimental value of power, power pulse rate, and efficiency are shown in Table 4. The average system efficiency achieved in simulation and experiment is 91.8% and 89.5%, respectively. Thus, it can be seen that the experimental results are similar to the simulation results as well as to the theoretical analysis.

To demonstrate the benefits of the proposed design system, design results are compared with other similar designs that have been performed in references [5], [6] as shown in Table 5.

The coil design method has been improved compared to the research [6]. In the proposed design, the coupling coefficient characteristic when the receiver moves with lateral misalignment is investigated, which is the basis for implementing advanced controls in the system. The power pulse rate of the method proposed (±9.5%) is larger than in [6] (±7.5%). However, it will continue to improve and can be flattened using the power control method.

Table 4. Simulation and experimental value of power and efficiency

Parameter	Simulation	Experimental
Average output power	1.4 kW	1.38kW
Power pulse rate	±10%	± 9.5%
Average system efficiency	91.8%	89.5%

Table 5. Compare the proposed design with other studies

Criteria	References[5]	References[6]	Proposed design
Application	Dynamic wireless charging for EV	Dynamic wireless charging for EV	Dynamic wireless charging for EV
Power	2.34 kW	1.4 kW	1.5 kW
Dimensions of transmission coil and receiving coil	72 x 27 cm 36 x 36 cm 20 turns	38.8 x 40 cm 48.5 x 40 cm 9 turns	40 x 40 cm 50 x 40 cm 10 turns
Air gap	10.5 cm	15 cm	15 cm
Coil design method	-	FEA	FEA
Coupling coefficient characteristic when EV moves lateral misalignment	No	No	Yes
Compensation circuit structure	LCC	LCC	LCC
Design the compensation circuit according to the optimal load value	Yes	No	Yes
Compensating circuit design considering coupling coefficient of transmission coils together	Yes (Complicate)	Yes (Simple)	Yes (Simple)
Working frequency	85 kHz	85 kHz	85 kHz
U_{DC}	300 V	180 V	310 V
U_{out}	-	150 V	400 V
The peak voltage stress on the compensation capacitor	-	1.3 kV	1.1 kV
The peak current on the compensation capacitor	-	40 A	26.1 A
SIC MOSFET	-	Yes	Yes
Average system efficiency	91.3 %	89.78 %	89.5 %
Power pulse rate	-	±7.5%	±9.5%

The designed LCC compensation circuit has the advantage that the transfer efficiency reaches the maximum value, the compensation circuit calculation method is simpler than in [5], the parameters of the compensation circuit are smaller than in [6]. This has practical implications in the design of large power systems. The efficiency in [5] is equal to 91.3%, which is larger than in the proposed design because of the larger size of the transmitter, the larger number of turns, and the smaller transfer distance.

4. Conclusion

The magnetic coupler is designed by the FEA method on Ansys Maxwell software. The coupling coefficient characteristic is analyzed in the case of the receiver moving with lateral misalignment, as a basis for the control to improve efficiency. The double-side LCC compensation circuit is designed according to the optimal load value to maximize the transfer efficiency and consider the coupling coefficient of the transmitting coils together. Small compensation circuit parameters are the basis of the design of high power systems. The experimental results show that the average output power is 1.38 kW, power pulse rate is ±9.5%. The average experimental system efficiency achieved 89.5%.

References

[1] Siqi Li and C. C. Mi, Wireless power transfer for electric vehicle applications, IEEE J. Emerg. Sel. Top. Power Electron., vol. 3, no. 1, pp. 4–17, Mar. 2015. https://doi.org/10.1109/JESTPE.2014.2319453

[2] S. Chopra, P. Bauer, Driving range extension of EV with on-road contactless power transfer - a case study, IEEE Trans. Ind. Electron., vol. 60, no. 1, pp. 329–338, Jan. 2013. https://doi.org/10.1109/TIE.2011.2182015

[3] J. M. Miller, P. T. Jones, J.-M. Li, O. C. Onar, ORNL experience and challenges facing dynamic wireless power charging of EV's, IEEE Circuits Syst. Mag., vol. 15, no. 2, pp. 40–53, 2015. https://doi.org/10.1109/MCAS.2015.2419012

[4] Y. Guo, L. Wang, Q. Zhu, C. Liao, F. Li, Switch-On Modeling and Analysis of dynamic wireless charging system used for electric vehicles, IEEE Trans. Ind. Electron., vol. 63, no. 10, pp. 6568–6579, Oct. 2016. https://doi.org/10.1109/TIE.2016.2557302

[5] Q. Zhu, L. Wang, Y. Guo, C. Liao, F. Li, Applying LCC compensation network to dynamic wireless EV charging system, IEEE Trans. Ind. Electron., vol. 63, no. 10, pp. 6557–6567, Oct. 2016. https://doi.org/10.1109/TIE.2016.2529561

[6] F. Lu, H. Zhang, H. Hofmann, C. C. Mi, A dynamic charging system with reduced output power pulsation for electric vehicles, IEEE Trans. Ind. Electron., vol. 63, no. 10, pp. 6580–6590, Oct. 2016. https://doi.org/10.1109/TIE.2016.2563380

[7] C.-S. Wang, O. H. Stielau, G. A. Covic, Design considerations for a contactless electric vehicle battery charger, IEEE Trans. Ind. Electron., vol. 52, no. 5, pp. 1308–1314, Oct. 2005. https://doi.org/10.1109/TIE.2005.855672

[8] S. Li, W. Li, J. Deng, T. D. Nguyen, C. C. Mi, A double-sided LCC compensation network and its tuning method for wireless power transfer, IEEE Trans. Veh. Technol., vol. 64, no. 6, pp. 2261–2273, Jun. 2015. https://doi.org/10.1109/TVT.2014.2347006

[9] V.-B. Vu, D.-H. Tran, W. Choi, Implementation of the constant current and constant voltage charge of inductive power transfer systems with the double-sided LCC compensation topology for electric vehicle battery charge applications, IEEE Trans. Power Electron., vol. 33, no. 9, pp. 7398–7410, Sep. 2018. https://doi.org/10.1109/TPEL.2017.2766605

[10] S. Li, C. C. Mi, Wireless power transfer for electric vehicle applications, IEEE J. Emerg. Sel. Top. Power Electron., vol. 3, no. 1, pp. 4–17, Mar. 2015. https://doi.org/10.1109/JESTPE.2014.2319453

[11] A. Berger, M. Agostinelli, S. Vesti, J. A. Oliver, J. A. Cobos, M. Huemer, A wireless charging system applying phase-shift and amplitude control to maximize efficiency and extractable power, IEEE Trans. Power Electron., vol. 30, no. 11, pp. 6338–6348, Nov. 2015. https://doi.org/10.1109/TPEL.2015.2410216

[12] W. X. Zhong, S. Y. Hui, Maximum energy efficiency tracking for wireless power transfer systems, Power Electron. IEEE Trans. On, vol. 30, pp. 4025–4034, Jul. 2015. https://doi.org/10.1109/TPEL.2014.2351496